

Damage evolution in adhesive joints subjected to impact fatigue

J.P. Casas-Rodriguez*, I.A. Ashcroft, V.V. Silberschmidt

Wolfson School of Mechanical and Manufacturing Engineering, Loughborough University, Leicestershire LE11 3TU, UK

Accepted 29 March 2007

The peer review of this article was organised by the Guest Editor

Available online 18 June 2007

Abstract

There is increasing interest in the effects of low-velocity impacts produced in components and structures by vibrating loads. This type of loading is known as impact-fatigue. The main aim of this paper is to investigate the behaviour of adhesive joints exposed to low-velocity impacting, to study the impact-fatigue life and to compare this loading regime with standard fatigue (i.e. non-impacting, constant amplitude, sinusoidal fatigue). To this effect, bonded aluminium single lap joints have been subjected to multiple impacting tensile loads and it has been shown that this is an extremely damaging load regime compared to standard fatigue. Two modifications of the accumulated time-stress model have been proposed to characterise the impact-fatigue results presented in this paper. The first model has been termed the *modified load-time model* and relates the total cumulative loading time of the primary tensile load wave to the mean maximum force. The second model attempts to characterise sample damage under impact-fatigue by relating the maximum force normalised with respect to initial maximum force to the accumulated loading time normalised with respect to the total accumulated loading time. This model has been termed the *normalised load-time model*. It is shown that both models provide a suitable characterisation of impact-fatigue in bonded joints.

© 2007 Elsevier Ltd. All rights reserved.

1. Introduction

In recent decades the use of structural adhesive joints in the aerospace industry has increased considerably thanks to their high strength-to-weight ratio, low stress concentration and capacity to joint different adherends [1].

The increase in structural applications of adhesive joints presupposes analysis of their fatigue behaviour, including the response of the adherends. Fatigue in an adhesive joint is more complicated than that in a homogeneous material and it should also be noted that the adhesive itself is usually a composite material [2]. Two main approaches have been used to analyse fatigue in bonded joints, namely the stress-life and fatigue crack growth-based methods [3]. In laboratory simulations, fatigue is generally approximated as a sinusoidal waveform, characterised by the stress ratio, i.e. the ratio between the minimum and maximum stress, frequency and the maximum stress. One of the main tools used to study fatigue based on the stress-life approach are S–N diagrams; representing the fatigue life dependence on stress. Their main limitation is the

*Corresponding author.

E-mail address: J.P.Casas-Rodriguez@lboro.ac.uk (J.P. Casas-Rodriguez).

lack of an explicit account of damage evolution during fatigue. The fatigue crack growth approach is used to characterise the crack growth per cycle (da/dn) with respect to some fracture mechanics parameters. In adhesives G_{\max} is commonly used, that is the strain energy release rate calculated at maximum load [2].

Studies of load time histories identify that aeromechanical parts generate vibrating loads [4] that can propagate into structural elements as cyclic impacts. This phenomenon is known as “impact-fatigue” [5]. Yu et al. [6], show that metals under impact-fatigue commonly have higher crack-growth rates than under standard fatigue (i.e. non-impacting, constant load amplitude, sinusoidal fatigue). The main features of impact-fatigue are high loading rates and the propagation of stress waves in components and structures. The former feature can be analysed experimentally using impacts at different velocities, while the latter can be studied via the effects of wave interaction. For instance, Maekawa [7] investigated the influence of stress waves in PMMA and concluded that the reason that short specimens had a shorter impact-fatigue life than long ones was because of the amplification effects caused by the superposition of stress waves.

Obviously, any analysis of multi-impact loading should be based on an understanding of the process in a single impact. Three main experimental configurations are commonly used in the analysis of impacts in adhesive joints. These are the pendulum test, the drop-weight test and the split Hopkinson bar test [8]. Two standard tests can be used to evaluate the impact strength in adhesives: ASTM D950:03 [9] and ISO 11343:03 [10]. The first of these involves two blocks that are bonded together. The bottom block is rigidly secured in the test rig and a pendulum hammer strikes the top block, thus generating a shear load in the adhesive layer. The second test is the impact wedge-peel test, in which a wedge loaded by a servo-hydraulic machine cleaves the joint, producing a peeling stress in the adhesive. Adams and Harris [11] analysed the block impact test and concluded that the stress condition is uncertain due to complex dynamic effects generated by uncertainties in the contact interface between the block and hammer. Blackman et al. [12] analysed the impact wedge-peel test and found that environmental conditions can generate different types of crack growth. Harris and Adams [1] proposed a test to measure impact strength in a single lap joint (SLJ) loaded by a tensile impact using a Charpy machine test. In a comparison of joints tested under impact and quasi-static loading, no conclusive trends could be seen. Similar results were also obtained by Beevers and Ellis [13]. Kihara et al. [14] designed a test to study the response of a thick adherend shear joint subjected to various impact stress waves and observed that the type of fracture was associated with the level of the incident stress.

In contrast to the vast body of research into impact loading of adhesive joints, impact-fatigue has received little attention to date. In many cases the analysis is limited to a relatively short series of impacts. Usui and Sakata [15] analysed impact-fatigue in GFRP SLJs bonded with an epoxy adhesive using a drop-weight test. Their results showed that the impact-fatigue strength of the joints was dependent on the magnitude of stress and loading time.

Researchers have also defined various empirical relations to be used to characterise impact fatigue. The most popular approach is to relate the cumulative time, $N_f T$, to the maximum stress amplitude in the impact, σ_{\max} , [6,16–18]:

$$\sigma_{\max} (N_f T)^m = C, \quad (1)$$

where N_f is the number of cycle to failure and T is the loading time, C and m are empirical impact-fatigue parameters. In this paper the relation described by Eq. (1) will be referred as the *accumulated time-stress model*.

Work has also been aimed at developing models to analyse impacts using fracture mechanics, specifically, the dynamic stress intensity factors K_d has been proposed as a suitable impact fracture criterion. Tsai et al. [19] found that under dynamic conditions, the relation between K and G depended on crack speed and that G_d is effectively constant with regard to crack speed almost to the Rayleigh wave velocity, at which point G_d increases rapidly. Fengchun et al. [20] suggested a method to define KI_d as a function of time $KI_d(t)$. This model was compared with experimental results and the results of finite-element analysis (FEA), demonstrating good accuracy for the loading history before crack initiation. Xie et al. [21] analysed KI_d experimentally and numerically using an in-house developed interface element that was implemented in commercial FEA software. The FEA results showed a good correlation with experimental data.

The current state of research into the impact-fatigue behaviour of adhesive joints is characterised by a lack of experimental studies of many facets of this phenomenon. This paper aims to provide one of the steps to cover this gap. It deals with a detailed experimental analysis of SLJs loaded by multiple tensile impacts.

Various characteristics of the joint response to such loading are studied and some new parameters to characterise the process are introduced. Results from standard fatigue tests are used as a basis for evaluating the danger of neglecting impact-fatigue in the durability analysis of components and structures.

2. Experimental procedures

2.1. Sample manufacture

Two types of SLJ have been used in this evaluation of impact-fatigue and standard fatigue in bonded joints (as shown in Fig. 1). Specimens were manufactured using aluminium 7075-T6 adherends and FM 73M adhesive. FM 73M is a single part rubber toughened, epoxy film adhesive with a non-woven polyester matrix carrier and is manufactured by Cytec Ltd. The material properties for the adhesive are given in Table 1 [22]. Fourteen samples were manufactured for impact-fatigue tests and ten to study standard fatigue. The latter testing was based on the ISO 9664:95[23].

The joint is manufactured in two stages. After grit blasting and degreasing the adherends a thin film of BR[®] 127 primer was applied to the bond area and dried for 30 min at room temperature. This is then cured at

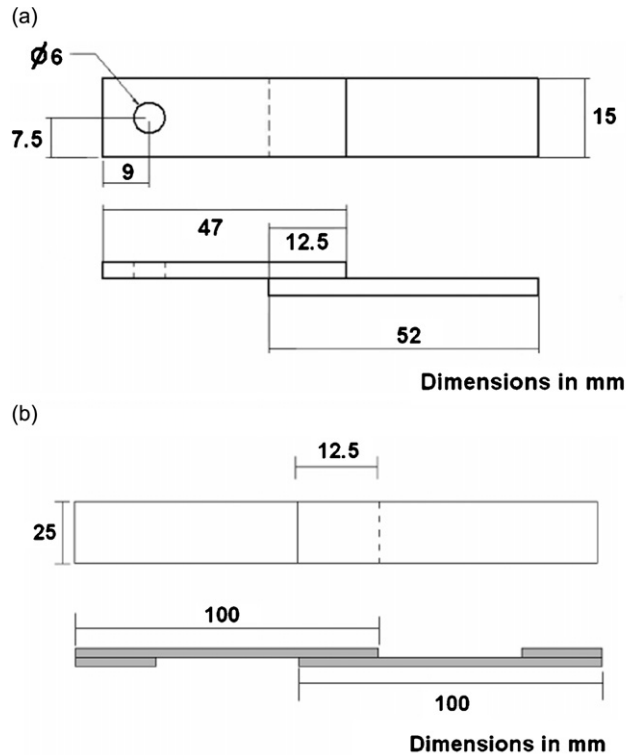


Fig. 1. Dimensions of lap strap joint specimens: (a) impact-fatigue specimen; (b) standard fatigue specimen.

Table 1
Mechanical properties of adhesive FM 73M

Conditions of the adhesive	Shear modulus (MPa)	Yield shear stress (MPa)	Ultimate shear stress (MPa)
24 °C, Dry	842	32.4	40.9

120 °C for 30 min. A sheet of FM 73 M is then cut into pieces of 12.5 mm × 26 mm. One piece of the cut adhesive is placed at the overlap between the adherends for each sample and any excess adhesive is cut off. Bonding is achieved by fixing the adherends using clamps and curing for 60 min at 120 °C. The adhesive thickness was measured after this process and found to be between 0.14 and 0.15 mm.

2.2. Impact-fatigue tests

Impact-fatigue was carried out using a modified CEAST RESIL impactor. The basis of this method is that a specimen (Fig. 2-2) is supported at one end in a vice (Fig. 2-7) and its opposite end is struck repeatedly by a controlled pendulum hammer, resulting in a dynamic uniaxial tensile loading. The specimen is clamped by the end with the circular hole to a specimen support (Fig. 2-4) using bolts (Fig. 2-5). A piezoelectric force transducer (Fig. 2-3) is also rigidly fixed to this support, and to the anvil (Fig. 2-6). At the free end of the specimen, a special impact block (Fig. 2-1) is fixed. This terminal block consists of a two plates held together by bolts. A firm connection between the specimen and impact block is obtained by compression of the plates. In addition, increased friction between the parts is obtained through an inscribed pattern on the surfaces of the plates.

The pendulum hammer that impacts the specimen was selected to transmit a maximum energy of 4 J. This corresponds to its initial position at an angle of 150° to the striking position. A pre-test analysis of mechanical friction existing between the mechanics parts and aero dynamical losses due to windage was implemented by measuring initial and final angles of the pendulum hammer in a single cycle without the specimen. This result is compared with the pre-established values that indicate the correct state of the testing machine and is automatically subtracted from the measured amount of energy dissipated in the specimen in each cycle of impact loading. The energy intervals used in the impact-fatigue tests ranged from 0.13 to 3.15 J, with the impact velocity ranging between 0.66 and 3.32 m/s. Variation in the magnitudes of the initial impact energy and velocity was achieved by changing the initial angle of the hammer. This is maintained during the impact-fatigue tests by automatic repositioning after braking in each cycle of loading.

In the impact-fatigue test, shown schematically in Fig. 3, the pendulum is released from a pre-selected initial angle that remains constant during an impact-fatigue test. Each impact produces a change in the electrical resistance of the piezo-electric sensor, which is captured by the data acquisition equipment. This signal is registered with a pre-selected sampling frequency of 833 kHz, with up to 8000 data points recorded per cycle. In order to decrease the data noise a 1 kHz filter was used. The amplified and filtered data was downloaded to a computer as magnitudes of force and time and this data is then used to calculate

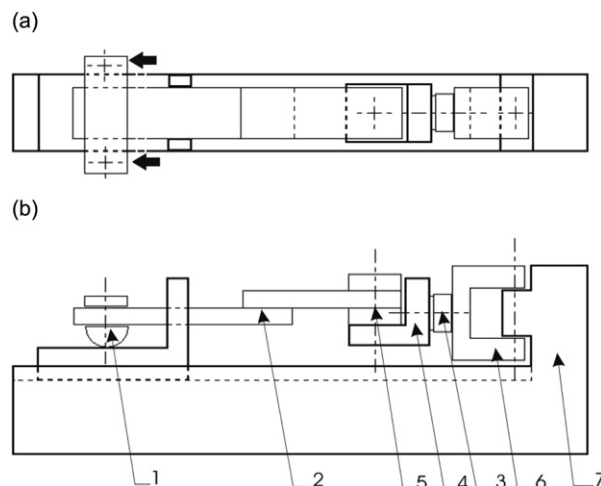


Fig. 2. Schematic of specimen fixture for impact fatigue: (a) top view, arrows denote impact application; (b) side view.

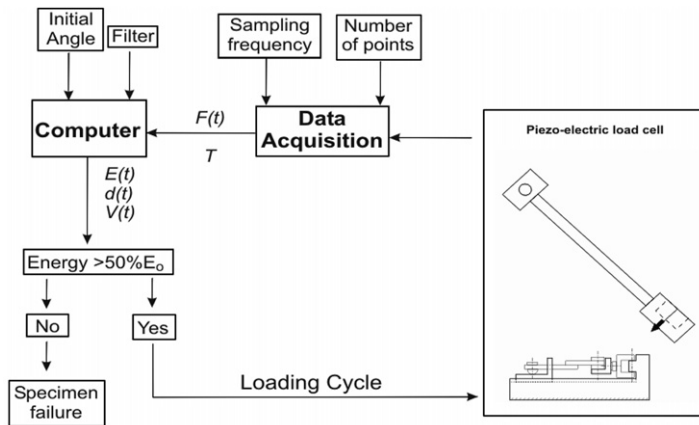


Fig. 3. Schematic of impact-fatigue test and data acquisition.

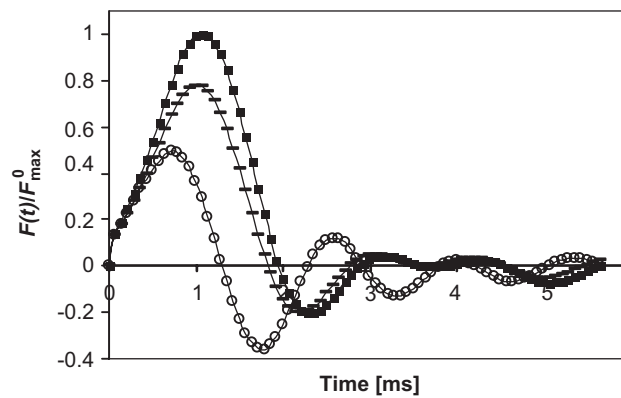


Fig. 4. Evolution of forces in specimen in various cycles of impact. ■ Initial impact, — penultimate impact, ○ last impact.

velocity V , displacement d and energy E for each impact. These parameters are calculated using the following relations:

$$V_i = V_{i-1} - \Delta t \left(\frac{F_{i-1} + F_i}{2m} - g \right), \tag{2}$$

$$d_i = d_{i-1} + \frac{\Delta t}{2} (V_{i-1} + V_i), \tag{3}$$

$$E_i = E_{i-1} + \frac{\Delta t}{2} [(FV)_{i-1} + (FV)_i], \tag{4}$$

where the index i is related to the current time and $i-1$ corresponds to the previous measurement, with the time difference Δt . The initial displacement and energy in Eqs. (3) and (4) are zero but the initial velocity V_o is calculated based on energy conservation during impact between the hammer and specimen.

In order to continue with the next impact, the impact-fatigue software first compares the maximum energy with the initial potential energy of the hammer, defining failure of the joint when this difference is higher than 50%. Typical graphs showing the evolution of the force response for impacts at various stages in a sample's life are shown in Fig. 4. It is obvious that the largest effect in a loaded joint is seen in the propagation of the first tensile wave. The influence of successive stress waves, caused by reflections from the edges and their

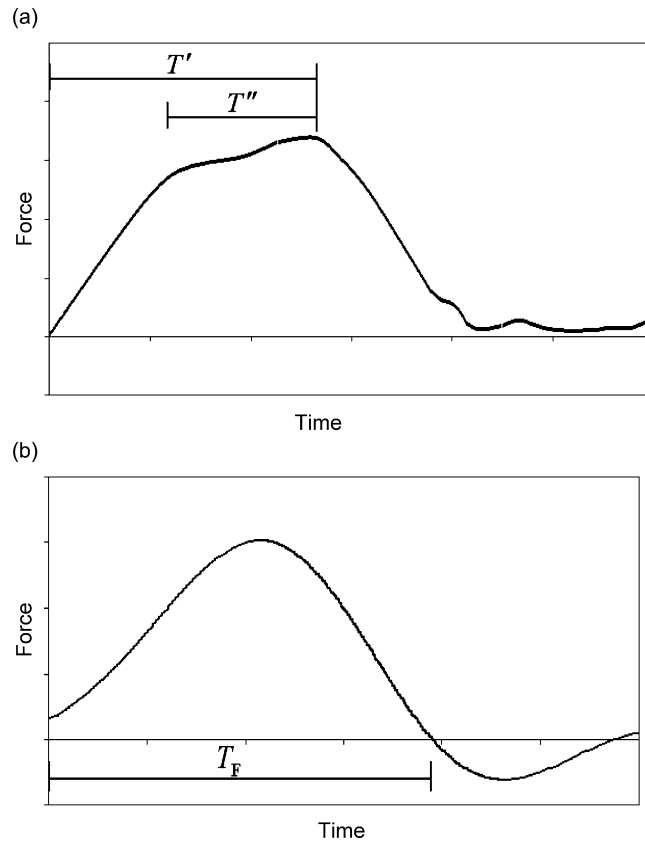


Fig. 5. Definitions of loading time: (a) Tanaka et al. model [16]; (b) current model.

interactions is considerably lower, being below 20% of the maximum force (F_{\max}). Damage is identified as deterioration of F_{\max} under continuing impact cycles and a drastic change is seen in the breaking impact (N_f).

To define the loading time T in Eq. (1), studies of impact have suggested various points in the graph of force vs. time. Tanaka et al. [16], defined the term T' as the time measured from the initial load change until the force begins to decrease after it has attained the maximum value (Fig. 5a). A second loading time was also proposed by Tanaka et al. [16], this being the time period when maximum force is applied, T'' (Fig. 5a). In this study, T_F is defined as the loading time and it represents the time to reach a zero force value from the initial loading point (Fig. 5b).

2.3. Standard fatigue

A servo-hydraulic fatigue testing machine utilising digital control and data logging was used in the standard fatigue tests. A load ratio (minimum load/maximum load) of $R = 0.1$ and frequency of 5 Hz was used in these tests, which were undertaken in load control in ambient laboratory environmental conditions. The same servo-hydraulic machine was also used to test specimens impact-fatigue and constant amplitude fatigue type samples (Fig. 1), under quasi-static loading conditions. In these tests a constant cross head speed of 0.3 mm/min was used.

3. Results and discussion

Following and modifying the standard S–N approaches introduced by Wöhler for fatigue, two types of diagrams are used in our study: load vs. number of cycles (F – N diagrams) and energy vs. number of cycles

(*E*–*N* diagrams). The *F*–*N* curve is used to analyse impact-fatigue in comparison to standard fatigue in the SLJs.

It is obvious from Fig. 4 that the function *F*(*t*) is not constant during the fatigue test. To overcome this obstacle, an additional parameter is introduced. The mean maximum force \bar{F}_{\max} is defined as

$$\bar{F}_{\max} = \frac{1}{N_f} \sum_{i=1}^{N_f} F_i^{\max}. \tag{5}$$

The mean maximum force in each specimen is normalised with respect to the maximum load supported by a similar specimen tested under quasi-static loading. The *F*–*N* plots in the standard fatigue tests exhibit three typical regions, as seen in Fig. 6. The first region showing little dependence on loading history until approximately 100 cycles, the failure load being similar to that under quasi-static conditions. The second region is a nearly linear relation between \bar{F}_{\max} and logarithm of the number of cycles to failure. The third stage is linked to an infinite life (durability limit), defined in this case at 10⁶ cycles at approx. 30% of the quasi-static strength. A similar analysis for impact-fatigue shows a drastic decrease in the fatigue life when specimens are loaded by multiple impacts. Measurements show that even for a considerably lower number of impacts, the strength of the joint is below 30% of the quasi-static strength. This shows that specimen tested in impact-fatigue conditions are more susceptible to failure, for a given maximum load, than those tested in standard fatigue.

The *E*–*N* fatigue curve is used to visualise the effect of multiple impacts on the life of joints in terms of energy. Changes in *F*(*t*) during an impact fatigue test also affect the energy absorbed by each impact, *E*_{*j*}^{*}. As *E*_{*j*}^{*} is not constant, new parameters are required to characterise impact-fatigue. The total energy absorbed during the entire life of the specimen up to its failure *E*_{*t*}^{*} is defined as

$$E_t^* = \sum_{j=1}^{N_f} E_j^*. \tag{6}$$

Here *E*_{*j*}^{*} is the amount of energy calculated using Eq. (4) for the entire duration of the *j*th impact. A specific energy (i.e. average absorbed energy per impact) can also be introduced as

$$\bar{E}_t = \frac{E_t^*}{N_f}. \tag{7}$$

The effect of specific energy on specimen life under impact-fatigue is shown in Fig. 7. This graph demonstrates a nearly linear relation between 0.5 and 3 J. Below approx. 0.2 J there is a change in gradient

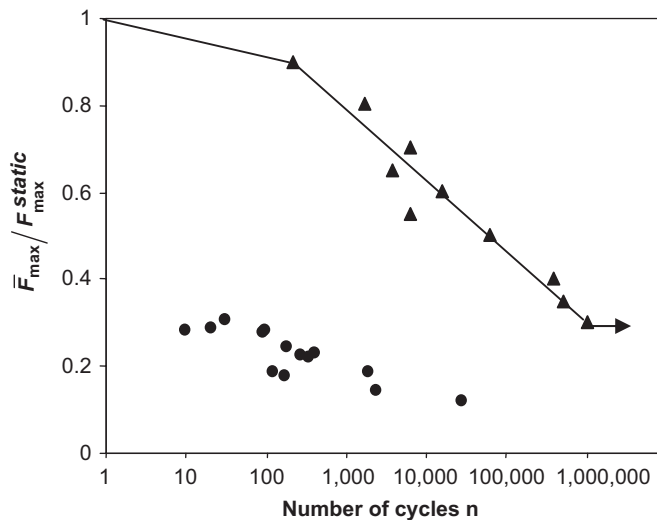


Fig. 6. *F*–*N* diagrams for aluminium joints for impact and standard fatigue. ● Impact fatigue, ▲ standard fatigue.

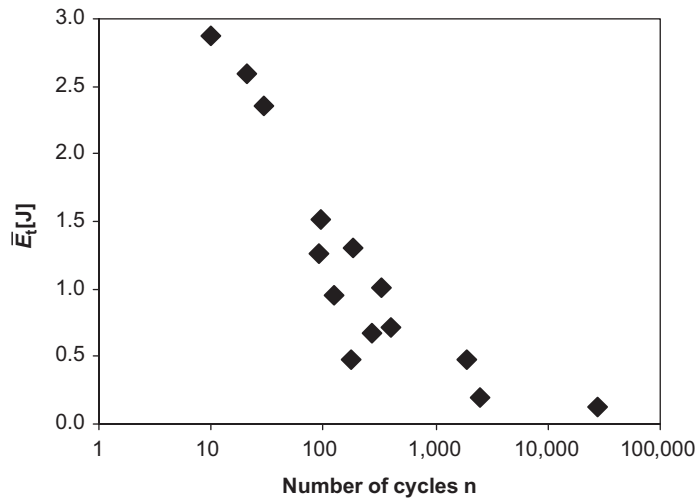


Fig. 7. E - N diagrams for impact fatigue.

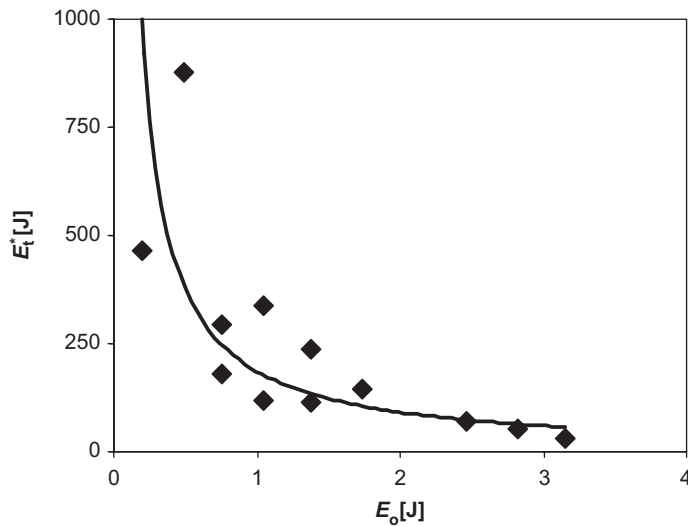


Fig. 8. Effect of initial energy of hammer on total energy.

with the curve becoming asymptotic to the x -axis. This graph shows what appears to be a fatigue threshold, however, this is at an extremely low proportion of the initial impact energy because of the severity of damage produced by this type of loading.

The total amount of energy that is necessary to break the joint, in impact-fatigue can be related to the level of initial potential energy E_o of the hammer at the beginning of each cycle, as shown in Fig. 8. This graph demonstrates that the total energy, E_i^* associated with failure of a specimen in impact-fatigue is not constant, but depends on E_o . As E_o increases there is a sharp decrease in E_i^* up to $E_o \approx 1$ J, after which E_i^* decrease more gradually. For values of E_o higher than 1 J the plot becomes asymptotic to the value at which a single impact will produce failure in the specimen. Additional experiments have shown that this will occur at $E_o \approx 4$ J.

Analysis of the specific energy, \bar{E}_i , demonstrates that this is also dependent on the initial energy, E_o . The parameter of energy restitution is defined as the ratio between \bar{E}_i and E_o , and represents the fraction of energy that a specimen can absorb on average, during impact-fatigue. This ratio is close to unity in the case when little changes occur to the initial energy during fatigue and there is no energy dissipation due to the relaxation

phenomena that can be present during impact. Obviously, it would be expected that in most cases the value of this parameter would be below 1. In the bonded joints test, the aluminium adherends are considerably stiffer than the adhesive and most of the energy dissipated in the system will be absorbed by the adhesive. Some part of the energy will be transformed into noise generated by the impact but previous research [15] indicates that this is negligibly small. In addition, as described above, losses due to mechanical and aerodynamic friction are automatically accounted for in the experimental measurements. All these facts support the idea that the capacity to dissipate energy in the system is directly related to the level of E_o (Fig. 9). Specifically, it is found that the response of the system is more inefficient at higher levels of energy.

Damage evolution in impact-fatigue can be analysed in terms of the deterioration of the maximum force and diminishing loading time. Typical curves showing the evolution of these parameters during an impact-fatigue test are shown in Fig. 10. These parameters are normalised with respect to the initial maximum force F_{max}^{10} and initial loading time T_F^{10} for the 10th impact. The 10th impact is used in order to avoid possible errors that can be introduced in the system by small misalignments between the pendulum hammer and the impact block in the initial stages of the experiment. It can be seen in Fig. 10 that the loading time decreases rapidly in the initial stages of fatigue but becomes more stable after approx. 10% of the fatigue life. The mean maximum force shows a sharp decrease initially and then continues a quasi-stable deterioration with fatigue life. With

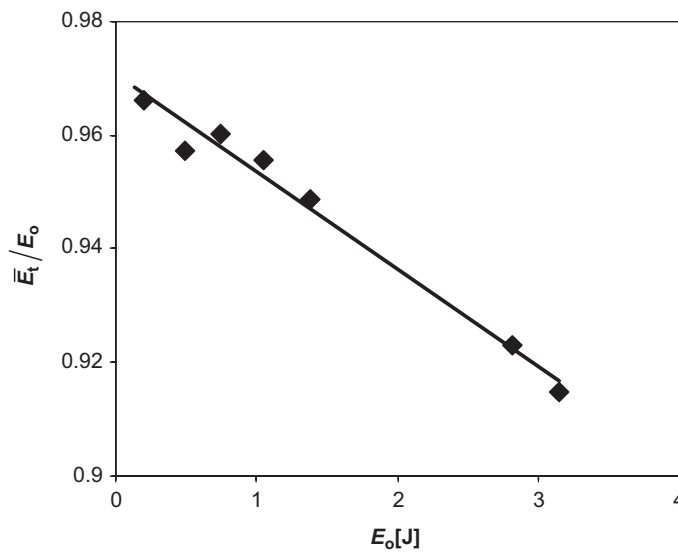


Fig. 9. Effect of initial energy on energy dissipation in impacts.

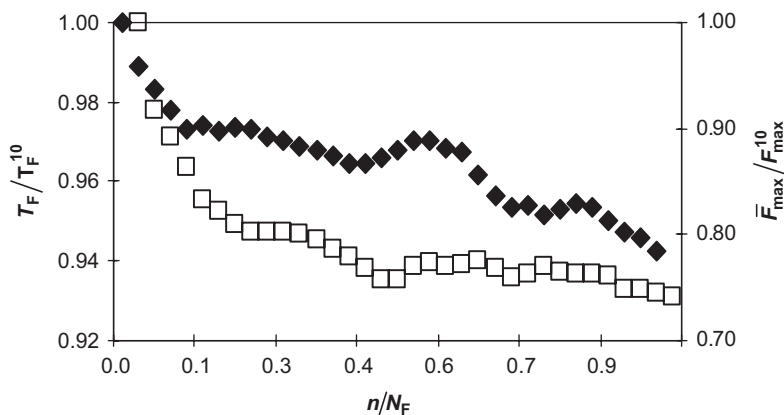


Fig. 10. Evolution of the relative values of maximum force and loading time during impact fatigue. □ Loading time, ◆ force.

regard to their initial values, it is seen that \bar{F}_{\max} decreases by some 20% during the test whilst diminishment in the loading time is considerably lower, at approx. 7%. This behaviour illustrates the deteriorating ability of the joint to withstand the impact, caused by damage evolution in the adhesive.

A modified version of the accumulated time-stress model, see Eq. (1), is proposed for the tests presented in this paper. This is because a re-definition of the original parameters in the loading time model is desirable to account for the observed variations in the loading time and maximum force. The total cumulative loading time, τ , is thus defined as

$$\tau = \sum_{i=1}^{N_f} T_{Fi}. \tag{8}$$

Using this definition and also the mean maximum force, \bar{F}_{\max} , the *modified load-time model* is presented as

$$\bar{F}_{\max} \tau^{m_1} = C_1. \tag{9}$$

The reason for using force, rather than stress, as in Eq. (1), is because of the highly non-uniform character of the stress distribution in the adhesive, in which stress concentrations are seen at the ends of the overlap, particularly close to the embedded corner of the adherend [24]. The model described by Eq. (9) is presented in Fig. 11, together with experimental data (where $m_1 = 0.087$ and $C_1 = 2344$). It can be seen in this figure that the modified load-time model presents a good characterisation of the fatigue behaviour of bonded lap joints subjected to impact-fatigue.

Another step in the analysis of impact-fatigue of joints is to identify if the accumulated loading time before the n th impact, τ_n , defined as

$$\tau_n = \sum_{i=1}^n T_{Fi} \tag{10}$$

is related to the decrease in the mean maximum force caused by damage accumulation in the specimen. Fig. 12 shows a linear decrease in the normalised maximum force with increasing τ_n (which is normalised with respect to τ). These results support the definition of a second model, termed the *normalised load-time model* that identifies the damage deterioration in a specimen as a result of impact-fatigue loading. In the model description in Eq. (11), the mean maximum force is normalised by the maximum force of the initial impact and as explained previously, for this analysis this was selected as 10th impact rather the first

$$\frac{\bar{F}_{\max}}{F_{\max}^{10}} \left[\frac{\tau_n}{\tau} \right]^{m_2} = C_2. \tag{11}$$

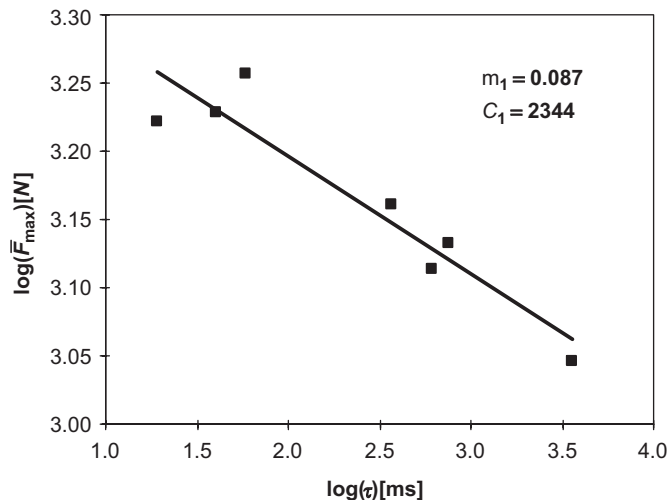


Fig. 11. Effect of the accumulated loaded time.

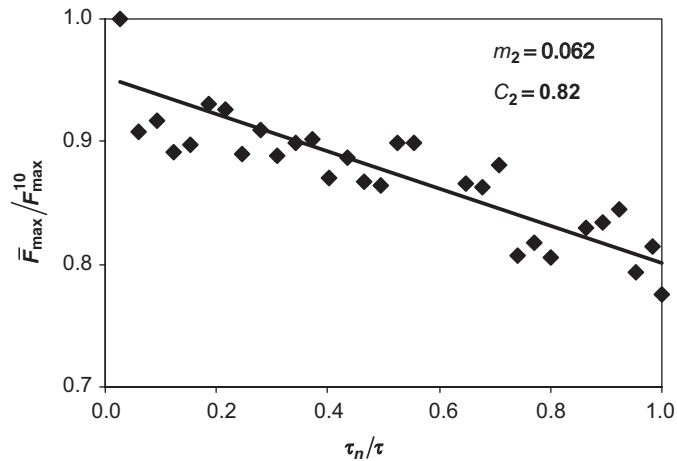


Fig. 12. Effect of accumulated loading time on damage evolution in joints.

4. Conclusions

Experimental results obtained from the impact-fatigue testing of bonded joints has clearly demonstrated the severity of damage produced by this type of loading and shown that it is more damaging than standard fatigue. Moreover, different trends are seen in load-life plots for the two types of loading. In standard fatigue a gradual decrease in the fatigue life with increasing load is seen whereas in impact-fatigue a significant decrease in life is seen at relatively modest maximum input forces after relatively few cycles. Comparisons of the fatigue life show a considerably earlier failure in impact-fatigue compared with standard fatigue when maximum force normalised with respect to quasi-static failure load is the charactering parameter.

$E-N$ curves, using the average accumulated energy \bar{E}_t , demonstrated the existence of an energy threshold, below which a significantly higher fatigue life can be expected, however this is at a much lower proportion of the initial strength than that seen in standard fatigue. An E_t^* limit of approx. 1 J was also observed, below which the specimen can be exposed to a long series of impacts.

It was found that the energy absorbing capacity of the joint is dependent on the level of E_o , with the response of the system being less efficient at higher levels of energy, which are linked to more pronounced and rapid damage accumulation. Impact-fatigue results also demonstrate that the maximum force per cycle and the loading time decrease as a result of damage to the sample during impacting.

Two modifications of the accumulated time-stress model have been proposed to characterise the impact-fatigue results presented in this paper. The first model has been termed the *modified load-time model* and relates the total cumulative loading time of the primary tensile load wave to the mean maximum force. The second model attempts to characterise sample damage under impact-fatigue by relating the maximum force normalised with respect to initial maximum force to the accumulated loading time normalised with respect to the total accumulated loading time. This model has been termed the *normalised load-time model*. It is shown that both models provide a suitable characterisation of impact-fatigue in bonded joints.

References

- [1] J.A. Harris, R.D. Adams, An assessment of the impact performance of bonded joints for use in high energy absorbing structures, *Proceedings of the Institution of Mechanical Engineers* 199 (1985) 121–131.
- [2] I.A. Ashcroft, A simple model to predict crack growth in bonded joints and laminates under variable-amplitude fatigue, *Journal of Strain Analysis* 39 (2004) 707–716.
- [3] I. Ashcroft, Fatigue, in: R.D. Adams (Ed.), *Adhesive Bonding*, Woodhead Publishing Limited, 2005, pp. 209–239.
- [4] J.O. Peters, R.O. Ritchie, Foreign-object damage and high-cycle fatigue of Ti-6Al-4V, *Journal of Materials Science and Engineering A* 319–321 (2001) 597–601.

- [5] I. Dumitru, S. Babeu, T. Babeu, Marsavina, Effect of prestressing on durability at repeated impacts. *Proceedings of the Euromech Colloquium*, 1998, pp. 261–274.
- [6] J. Yu, K. Peter, M. Huang, The impact-fatigue fracture of metallic materials, *JOM* 51 (1999) 15–18.
- [7] I. Maekawa, The influence of stress wave on the impact fracture strength of cracked member, *International Journal of Impact Engineering* 32 (2005) 351–357.
- [8] C. Sato, Impact behaviour of adhesively bonded joints, in: R.D. Adams (Ed.), *Adhesive Bondings*, Woodhead Publishing Limited, 2005, pp. 164–188.
- [9] ASTM D950-2003, Standard test method for impact strength of adhesive bonds.
- [10] ISO 11343:2003, Adhesives. Determination of dynamic resistance to cleavage of high-strength adhesive bonds under impact conditions, wedge impact method.
- [11] R.D. Adams, J.A. Harris, A critical assessment of the block impact test for measuring the impact strength of adhesive bonds, *International Journal of Adhesion and Adhesives* 16 (1996) 61–71.
- [12] B.R.K. Blackman, A.J. Kinloch, A.C. Taylor, Y. Wang, The impact wedge peel performance of structural adhesives, *Journal of Material Science* 35 (2000) 1867–1884.
- [13] A. Beevers, M.D. Ellis, Impact behaviour of bonded mild steel lap joints, *International Journal of Adhesion and Adhesives* 4 (1984) 13–16.
- [14] K. Kihara, H. Isono, H. Yamabe, T. Sugibayashi, A study and evaluation of the shear strength of adhesive layers subjected to impact loads, *International Journal of Adhesion and Adhesives* 23 (2003) 253–259.
- [15] Y. Usui, O. Sakata, Impact-fatigue strength of adhesive joints, *Precise Machinery* 48 (1982) 498–502 (in Japanese).
- [16] M. Ninomi, K. Uwai, T. Kobayashi, A. Okahara, Impact fatigue properties of epoxy resin filled with SiO₂ particles, *Engineering Fracture Mechanics* 38 (1991) 439–449.
- [17] I. Yamamoto, T. Higashihara, T. Kobayashi, Effect of silica-particle characteristics on impact/usual fatigue properties and evaluation of mechanical characteristics of silica-particle epoxy resins, *Japanese Society of Mechanical Engineers, Series A* 46 (2003) 145–153.
- [18] T. Tanaka, K. Kinoshita, H. Nakayama, Effect of loading time on high-cycle range impact-fatigue strength and impact-fatigue crack growth rate, *Japan Society of Mechanical Engineers, Series I* 35 (1992) 108–116.
- [19] J.L. Tsai, C. Guo, C.T. Suna, Dynamic delamination fracture toughness in unidirectional polymeric composites, *Composite Science and Technology* 61 (2001) 87–94.
- [20] J. Fengchun, L. Ruitang, Z. Xiabin, K. Vecchio, A. Rohatgi, Evaluation of dynamic fracture toughness KI_d by Hopkinson pressure bar loaded instrumented Charpy impact test, *Engineering Fracture Mechanics* 71 (2004) 279–297.
- [21] D. Xie, Calculation of transient strain energy release rates under impact loading based on the virtual crack closure technique, *International Journal of Impact Engineering*, in press. Corrected proof, available online 11 May 2006.
- [22] Cytec Engineering Materials, Data sheet of FM 73, Cytec Engineering Materials, 1998.
- [23] ISO 9664:1995, Adhesives. Test methods for fatigue properties of structural adhesives in tensile shear.
- [24] M.M. Abdel Wahab, A.D. Crocombe, A. Beevers, K. Ebtehaj, Coupled stress-diffusion analysis for durability study in adhesively bonded joints, *International Journal of Adhesion and Adhesives* 22 (2002) 61–73.